A Diffuse Reflectance Comparative Study of Benzil Inclusion within *p-tert*-Butylcalix[*n*]arenes ($n = 4$, 6, and 8) and Silicalite

L. F. Vieira Ferreira,*,† I. Ferreira Machado,† A. S. Oliveira,† M. R. Vieira Ferreira,‡ J. P. Da Silva,†,§ and J. C. Moreira[||]

Centro de Química-Física Molecular-Complexo Interdisciplinar, Instituto Superior Técnico, Av. Rovisco Pais, 1049-001 Lisboa, Portugal, Secção de Química Orgânica, Departamento de Engenharia Química, Instituto Superior de Engenharia de Lisboa, R. Conselheiro Emídio Navarro, 1949-014 Lisboa, Portugal, FCT, Universidade do Algarve, Campus de Gambelas, 8000 Faro, Portugal, and Centro de Estudos da Saúde do Trabalhador e Ecologia Humana, ENSP, Fundação Oswaldo Cruz, Rua Leopoldo Bulhões 1480, Rio de Janeiro, RJ, 21041-210, Brazil

Received: July 22, 2002; In Final Form: October 3, 2002

Diffuse reflectance and laser-induced techniques were used to access photochemical and photophysical processes of benzil in solid supports, namely *p-tert*-butylcalix[*n*]arenes with $n = 4$, 6, and 8. A comparative study was performed using these results and those obtained with another electronically inert support, silicalite, which is a hydrophobic zeolite. In the latter substrate, ground-state benzil has the two carbonyl groups in an *s*-trans planar conformation while in the calixarenes a distribution of conformers exists, largely dominated by skew conformations where the carbonyl groups are twisted one to the other. In all substrates, room-temperature phosphorescence was obtained in air-equilibrated samples. The decay times vary greatly and the largest lifetime was obtained for benzil/*p-tert*-butylcalix[6]arene, showing that this host cavity well accommodates benzil, enhancing its room-temperature phosphorescence. *p-tert*-Butylcalix[6] and [8]arene molecules provide larger hydrophobic cavities than silicalite, and inclusion complexes are formed with these hosts and benzil as guest; *p-tert*-butylcalix[4]arene does not include benzil. This probe is deposited outside the calix[4] cavity, in the form of microcrystals. Triplet−triplet absorption of benzil was detected in all cases and is predominant in the silicalite channel inclusion case. Benzil ketyl radical formation occurs with inclusion in calix[6]arene and calix[8]arene. In the three cases, benzoyl radical was detected at long times (in the millisecond time scale). Product analysis and identification clearly show that the main detected degradation photoproducts in all substrates are benzoyl radical derivatives. Calix[6] and [8]arenes are able to supply hydrogen atoms that allow also another reaction, the reduction to benzoin through benzil ketyl radical formation.

1. Introduction

p-tert-Butylcalixarene molecules are cyclooligomers containing phenolic units linked by methylene bridges forming macrocycles. These calix molecules provide cavities with different sizes with a polar lower rim and a nonpolar upper rim.[1−4] These molecules have some internal mobility, so conformational isomerism is an important characteristic of these compounds.[5,6] Their ability to form inclusion complexes, accommodating guest molecules or ions in their intramolecular cavities, greatly depends on the size and geometry of both guest molecule and host cavity.[5,7,8]

Owing to their characteristics and selectivity, calixarenes appear to be very useful substrates for photochemical studies.[9] Calix[*n*]arenes (mainly those with $n = 4$, 6, and 8) have recently received considerable interest due to their ability to form inclusion complexes both with organic molecules and ions, either in water or organic solvents with reasonable selectivity.[6−8] For this reason they have been used in many areas such as catalysis, separation, and analysis.[4−8]

* Author to whom correspondence should be addressed. Tel.: 351-21 841 92 52. Fax: 351-21 846 44 55. E-mail: LuisFilipeVF@ist.utl.pt.
† Instituto Superior Técnico.
‡ Instituto Superior de Engenharia de Lisboa.
§ Universidade do Algarve.
|| Centro de Estudos da Saúde do Trabalhador e Ecologia Humana, ENSP.

SCHEME 1

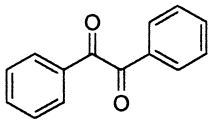

Benzil (BZL)

Despite the extended use of this family of compounds as hosts for inclusion complex formation, calixarenes have received much less attention from photochemists when compared with other host molecules of practical importance, even in solution studies. Very few photochemical studies of organic compounds within calixarenes were presented.[9−15]

Benzil (Scheme 1) is an extremely useful molecule for probing new hosts. Being a α-dicarbonyl compound it presents different conformations due to rotation of the central carbonyl−carbonyl bond in the ground and excited states.[16−21] In the ground-state it has a nonplanar (skew) conformation, the twist angle of the two benzoyl moieties being about 72°. Upon excitation, in fluid media, both the first excited singlet state and the first excited triplet state have relaxed to an identical conformation, i.e., to a *s*-trans planar geometry in which the −CO−CO− dihedral angle is 180°.[17,19] Therefore, both fluorescence and phosphorescence are dependent on external

10.1021/jp021685n CCC: $22.00
Published on Web 11/13/2002

constraints imposed by the environment. Benzil has a $n \rightarrow \pi^*$ absorption transition and was found to have zero or near-zero dipole moment in the triplet state in benzene solution, thus confirming the *s*-trans structure of the excited state.[19]

The solution photochemical reactions of benzil were studied both by flash photolysis[20] and time-resolved electron spin resonance.[21] Benzoyl and benzil ketyl radicals were detected.

Silicalite is a de-aluminated analogue of ZSM-5 zeolite. The lack of substitutional aluminum results in silicalite having no catalytic or exchange properties compared with the ZSM-5 zeolites. Silicalites are the only known hydrophobic forms of silica capable of adsorbing organic molecules up to about 6 Å of kinetic diameter, even removing them from water.[22]

Ground-state diffuse reflectance absorption spectroscopy, time-resolved laser induced luminescence, and diffuse reflectance laser flash-photolysis are relatively new techniques that can be applied to study opaque and crystalline systems.[23−26] These solid-state photochemical methods have been applied to the study of several organic compounds adsorbed or included in many solid powdered substrates such as microcrystalline cellulose,[27] silicalite, silica, cyclodextrins, and clays. Properties and applications of such solid substrates are described elsewhere.[23−28]

In this paper we present a diffuse reflectance and laser-induced fluorescence study of benzil included into *p-tert*-butylcalix[*n*]arenes with $n = 4$, 6, and 8. These results will be compared with those obtained with another electronically inert host, silicalite, a hydrophobic zeolite.

2. Experimental Section

Materials. *p-tert*-Butylcalix[4], [6], and [8]arenes (all from Aldrich) were used without further purification. Benzil, also from Aldrich, was recrystallized from ethanol. Chloroform, isooctane, and ethanol (Merck, Uvasol grade) were used as received. Silicalite was purchased from Union Carbide. Benzoin and benzaldehyde used as authentic samples were from Aldrich, biphenyl from Eastman-Kodak (highest purity available), and benzophenone from Koch-Light (Scintillation grade). 60 Å pore silica, neutral Al_2O_3, and zeolite Y were purchased from Aldrich.

Sample Preparation. The samples used in this work were prepared using the solvent evaporation method. This method consists of the addition of a solution containing the probe to the previously dried or thermally activated powdered solid substrate, followed by solvent evaporation from the stirred slurry in a fume cupboard. The final solvent removal was performed overnight in an acrylic chamber with an electrically heated shelf (Heto, model FD 1.0-110) with temperature control (30 ± 1 °C) and under moderate vacuum at a pressure of ca. 10^{-3} Torr. The evaluation of the existence of final traces of solvent was monitored by the use of FTIR spectra.

For calixarenes, the solid complexes ketone−calixarene of molar ratios 1:1, 1:2.5, 1:5, and 1:10 were prepared by mixing a saturated solution of the calixarene in chloroform ($\sim 10^{-2}$ M of *p-tert*-butylcalix[4], *p-tert*-butylcalix[6], and *p-tert*-butylcalix[8]arenes) and a solution of the ketone in the same solvent. The resulting mixture was magnetically stirred for at least 24 h and then allowed to evaporate in a fume cupboard. Finally, the samples were dried under reduced pressure.

For silicalite samples, benzil selective adsorption into the silicalite channels was achieved using isooctane, whose molecular dimensions prevent this solvent from penetrating into the host channels. Following the initial solvent evaporation, samples were washed three times with isooctane for complete removal of the nonincluded ketone and dried again as described. Ground-state absorption studies revealed that for 100, 250, 500, and 1000 μmol g^{-1} samples, the amount of ketone deposited onto the silicalite surface does not exceed 5%.

Methods. *1. Diffuse Reflectance Ground-State Absorption Spectra (GSDR).* Ground-state absorption spectra for the solid samples were recorded using an OLIS 14 spectrophotometer with a diffuse reflectance attachment. Further details are given elsewhere.[23,24,27]

2. Diffuse-Reflectance Laser Flash Photolysis (DRLFP) and Laser-Induced Luminescence (LIL) Systems. Schematic diagrams of the DRLFP system and of the LIL systems are presented in refs 23 and 29. Laser flash photolysis experiments were carried out with the third or the fourth harmonic of a YAG laser (355 and 266 nm, ca. 6 ns fwhm, ∼10−30 mJ/pulse) from B. M. Industries (Thomson-CSF, model Saga 12−10), in the diffuse reflectance mode.[9,23] The light arising from the irradiation of solid samples by the laser pulse is collected by a collimating beam probe coupled to an optical fiber (fused silica) and is detected by a gated intensified charge-coupled device (ICCD, Oriel model Instaspec V). The ICCD is coupled to a fixed imaging compact spectrograph (Oriel, model FICS 77440). The system can be used either by capturing all light emitted by the sample or in a time-resolved mode by using a delay box (Stanford Research Systems, model D6535). The ICCD has high-speed (2.2 ns) gating electronics and intensifier and covers the 200−900 nm wavelength range. Time-resolved absorption and emission spectra are available in the nanosecond to second time range.[9,23] Transient absorption data are reported as percentage of absorption (% Abs), defined as $100\Delta J_t/J_o = (1 - J_t/J_o)100$, where J_o and J_t are diffuse reflected light from the sample before exposure to the exciting laser pulse and at time t after excitation, respectively.[9,23]

For the laser-induced luminescence experiments, a N_2 laser (PTI model 2000, ca. 600 ps fwhm, ∼1.3 mJ per pulse) was also used.

For kinetic studies (decay curves at a specific wavelength), a more simple system was used, based in a Hamamatsu photomultiplier (model R955) as detector, coupled to an analyzing monochromator (Oriel, model 77250 with 77298 grating). The luminescence obtained after exciting the solid powdered samples with the laser pulse (266, 337, or 355 nm) was collected by a collimating beam probe coupled to an optical fiber bundle (fused silica). The signal was amplified with a preamplifier (Oriel, model 70723, 350 MHz) and Thorn EMI Electron Tubes A1 and/or A2 amplifiers. Decay curves were obtained with the use of a 8 bits AD-converter/recorder system (Fast, model TR50, 50 MHz), and each curve was the average of at least 50 decays.

3. Infrared Spectroscopy (FTIR). Infrared spectra were recorded with a Nicolet Impact 400D FTIR spectrometer in transmittance mode by the use of KBr pellets. Spectra were recorded at 1.0 cm^{-1} resolution, in the range 4000−500 cm^{-1} as a ratio of 36 single-beam scans of the sample to the same number of background scans from air. Baseline corrections were introduced whenever needed. The original samples were diluted in KBr (ca. 2% w/w) and ground to a finely divided powder with the use of an agate mortar and pestle.

4. Irradiation and Product Analysis. Photodegradation studies were conducted in a reactor previously used to study the photochemistry of pesticides.[30] The samples were irradiated at 254 nm using a 16 W low-pressure mercury lamp (Applied Photophysics) without filters and without refrigeration. The photodegradation products were extracted by washing the irradiated samples with methanol or ethanol. Photolysis was

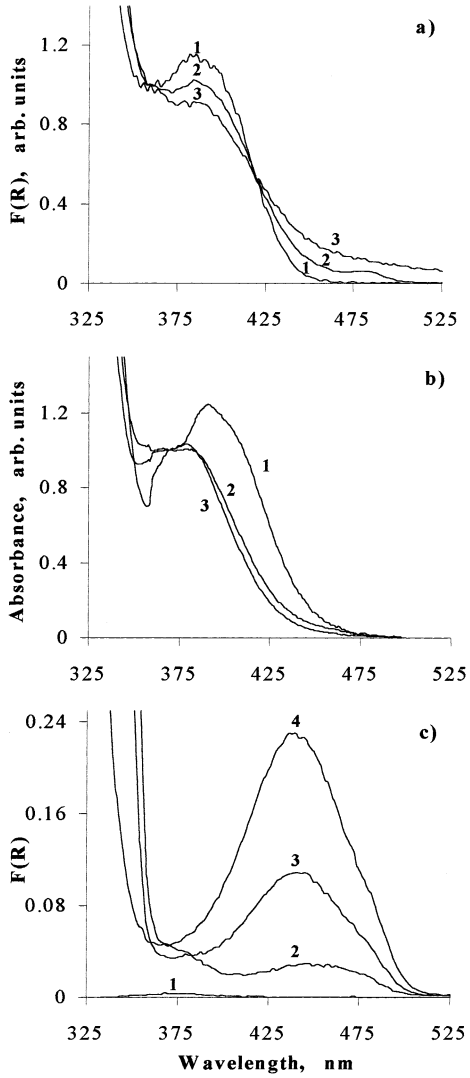

Figure 1. (a) Remission function for benzil/calix[4]arene sample and benzil/calix[*n*]arene inclusion complexes for $n = 6$ and 8 (molar ratio of 1:2.5), curves 1, 2, and 3, respectively. The remission function is normalized to unity at 360 nm. (b) Solution absorption spectra for benzil in hexane (curve 1), ethanol (curve 2), and acetonitrile (curve 3) normalized at 360 nm. (c) Remission function for benzil/silicalite samples with concentrations of 100, 250, and 500 μmol g^{-1} (curves 2, 3, and 4, respectively) and also for the substrate (curve 1).

followed by HPLC using a Merck-Hitachi 655A-11 chromatograph with a 655A-22 UV detector. Analyses were conducted at conversions lower than 10%. UV−Vis spectra of the degradation products were obtained using the same HPLC system but with a diode array detector (Shimadzu, SPD-M6A). Mass spectra were obtained by GC-MS using a Hewlett-Packard 5890 Series II gas chromatograph with a 5971 Series mass selective detector (E.I. 70 eV).

3. Results and Discussion

Ground-State Diffuse Reflectance and Infrared (FTIR) Absorption Spectra. Figure 1a shows the ground-state electronic absorption spectra of samples of benzil and *p-tert*-butylcalix[4], [6], and [8]arene ($n \rightarrow \pi^*$ transition only, with absorption maxima wavelengths around 387 nm).

No remarkable sharp differences can be seen in this set of spectra, and only small shifts can be detected, in contrast with the ground-state absorption spectra of benzophenone inclusion complexes formed with the same hosts as described in ref 9. The $n \rightarrow \pi^*$ absorption region of benzil does not present a clear vibronic structure, but rather a nonstructured and broad band in these hosts. This broadening effect increases with the increase of the calixarene size, suggesting that the larger the calixarene cavity is, the larger is the number of different ground-state conformers of benzil formed, namely those approaching planarity. At the same time, the wavelength maximum absorption deviates from 391 nm in calix[4] to 387 nm in calix[6] and to 384 nm in calix[8], in accordance with the increase in polarity of the host as reported in ref 9 ($n \rightarrow \pi^*$ transition deviates to the blue with increasing polarity).

For comparison purposes, solution spectra of benzil are presented in Figure 1b. The effect of increasing polarity on the $n \rightarrow \pi^*$ absorption transition going from hexane to a polar aprotic solvent as acetonitrile or polar protic as ethanol is also quite clear (hypsochromic shift) as curves 3 and 2 show. Polar solvents stabilize preferentially the ground state rather than the excited state and absorption spectra are deviated hypsochromically. Upon excitation, benzil molecules undergo extensive conformational reorganization. The ground-state dipole moment is 3.75 D, and the excited-state dipole moment is zero.[19]

Figure 1c shows the remission function spectra obtained for 100, 250, and 500 μmol g^{-1} of benzil included within silicalite channels, as well as the substrate absorption within the same wavelength range (curve 1). As described before, this host has internal elliptical channels (5.4 × 5.6 Å axis) where probes may enter, and the surface internal area (about 1000 m^2 per gram) is by far larger than the external area.[31] A new absorption band of benzil peaking at 442 nm becomes predominant in this case, which we assign as *s*-trans planar ground-state conformers of this α-dicarbonyl molecule. The dimensions of silicalite channels are large enough for benzil to enter these cavities, but at the same time they are small enough to impose severe conformational restrictions, in this case forcing the benzil molecules to assume a *s*-trans planar conformation. Silicalite allows an axial motion, increasing planarity of the carbonyl groups, as the molecule can rotate along the central C−C bond. As a consequence of this increase of planarity of the carbonyl groups, less energy is required for the $n \rightarrow \pi^*$ transition to occur and a new band peaking at 442 nm appears, with a ca. 50 nm bathochromic shift relative to the same transition in solution or in the calixarenes case.

Another possible interpretation for the new absorption band centered at 442 nm could be a charge-transfer band attributed to a charge-transfer complex (CT complex). Benzil could act as an electron donor and the Lewis acid surfaces sites of silicalite could act as the electron acceptor (or even sites with O_2 on the internal surface of silicalite could be acceptors). Biphenyl and pyrene were reported to exhibit CT bands on the surface of activated γ-alumina (activation temperature of 750 °C) or clays.[32,33] In our case, however, this explanation is not suitable, because our activation temperatures were much smaller than those used in the above-mentioned cases and, most of all, silicalite has a very small percentage of aluminum in its structure, reason for its hydrophobic character. So, the number of active Lewis sites is reduced and CT interactions are therefore diminished when compared to the ZSM-5 analogue. Two other samples of 500 μmol g^{-1} were prepared to test this hypothesis: benzil adsorbed on ZSM-5 provided ground-state absorption spectra similar to silicalite samples; benzil on silica with 60 Å pores showed a normal $n \rightarrow \pi^*$ transition, peaking at about 380 nm. Both facts corroborate the explanation of the channel structure imposing conformational restrictions and not the CT character of the transition. At the same time, air-equilibrated

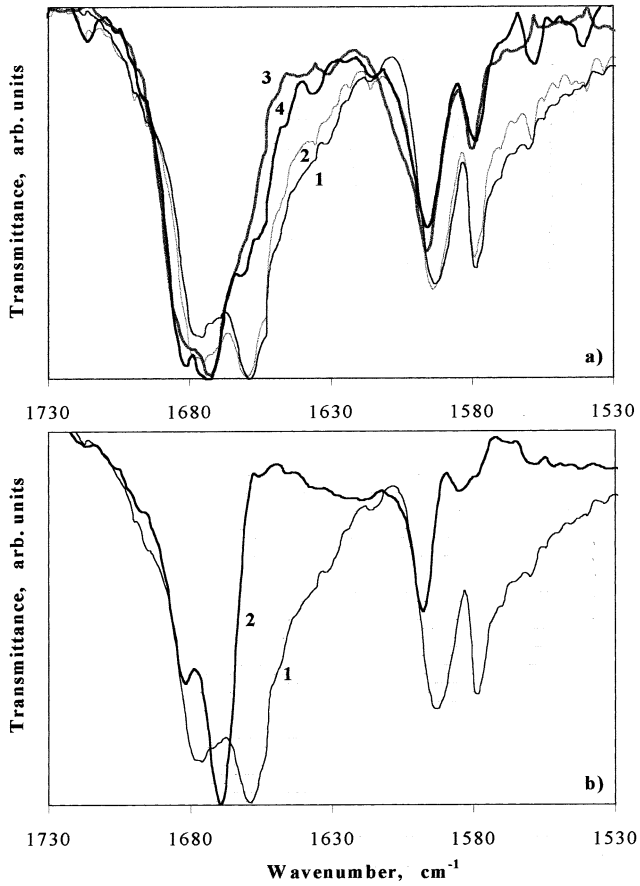

Figure 2. Transmission FTIR absorption spectrum of (a) microcrystals of benzil (curve 1) and benzil/calix[4]arene sample and benzil/calix-[*n*]arene inclusion complexes for $n = 6$ and 8 (curves 2 to 4, respectively) with a 1:1 molar ratio in a KBr matrix. (b) Microcrystals of benzil (curve 1) and benzil/silicalite 500 μmol g^{-1} (curve 2) also in a KBr matrix. All spectra are normalized to the maximum of the carbonyl stretching band.

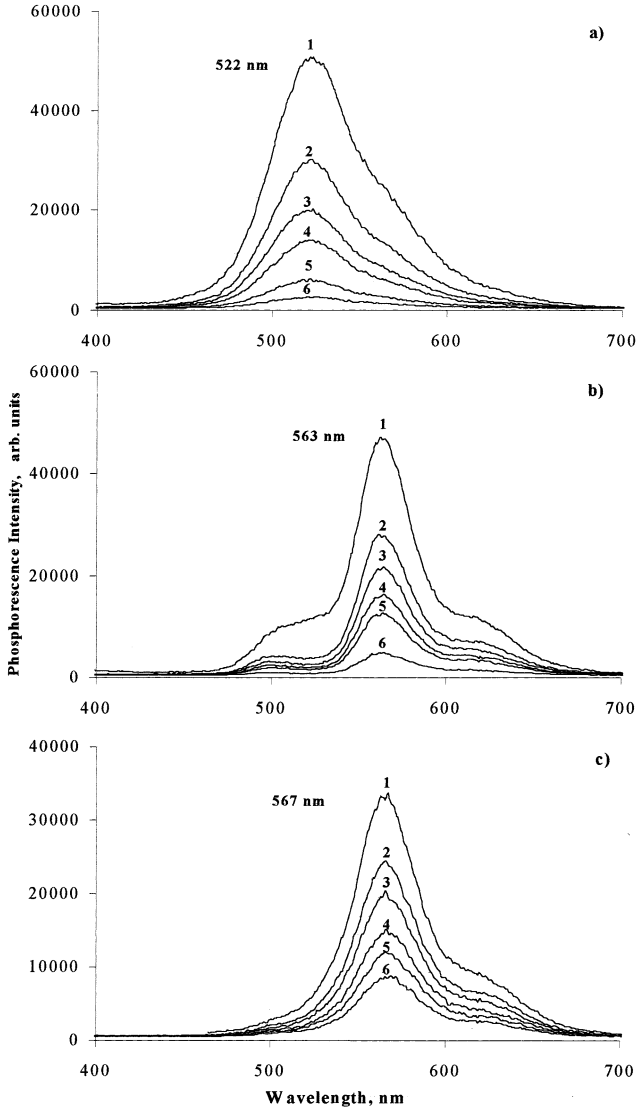

Figure 3. Room-temperature laser-induced phosphorescence emission spectra from argon-purged samples of (a) benzil/calix[4]arene sample (molar ratio 1:2.5). Curves 1, 2, 3, 4, 5, and 6 were recorded 0.1, 50, 100, 150, 250, and 450 μs after laser pulse. (b) Benzil/calix[6]arene inclusion complex (molar ratio 1:2.5). Curves 1, 2, 3, 4, 5, and 6 were recorded 0.1, 250, 500, 750, 1000, and 2000 μs after laser pulse. (c) Benzil/calix[8]arene inclusion complex (molar ratio 1:2.5). Curves 1, 2, 3, 4, 5, and 6 were recorded 0.1, 25, 50, 100, 150, and 225 μs after laser pulse. $\lambda_{exc} = 337$ nm in all cases.

or argon-purged silicalite samples provided the same ground-state diffuse reflectance spectra.

Another strong argument for the assignment of the 442 nm absorption band of benzil within silicalite as originating from *s*-trans planar conformers comes from the emission of the frozen sample (77 K), where ground-state conformations are kept. The phosphorescence emission obtained at 77 K is similar to the room temperature emission of Figure 4a, peaking at 563 nm. Only a large increase in the lifetime was detected (τ_P(77 K) $\approx$ 1.5 ms), as expected. The emission from frozen hexane and acetonitrile solutions of benzil exhibit *s*-cis conformational behavior, peaking at about 525 nm, in accordance with data reported for other solvents.[17a] As expected for predominant ground-state *s*-cis conformations, samples of benzil adsorbed onto Al_2O_3, 60 Å pore silica, or zeolite Y (500 μmol g^{-1} in all cases), present ground-state absorption spectra similar to the one obtained for calix[4]arene.

The second major information regarding the geometry of the benzil molecule within the calixarenes and silicalite came from FTIR spectra. Table 1 presents data of the carbonyl stretching wavenumbers obtained from FTIR absorption spectra for samples of microcrystals of benzil, benzil/calix[*n*]arene ($n =$ 4, 6, and 8) and benzil/silicalite samples.

The double absorption of the carbonyl, reported in the literature,[35] is due to the angle the carbonyls form one to the other and also with the phenyl groups in the ground state.[17b] So, the carbonyl stretching bands in benzil microcrystals are located at 1676 and 1659 cm^{-1}. Inclusion into calix[6]arene, calix[8]arene, and silicalite results in a clear increase in the energy of the C═O stretching mode due to the C═O double bond character enhancement (inclusion of the calixarenes into cavities promote deviations from planarity in the phenyl−carbonyl conjugated system, therefore decreasing resonance). It is also quite evident from Table 1 that benzil is not included into the calix[4]arene cavity, since the frequencies of the carbonyl stretching bands are very similar to the ones of benzil microcrystals.

Curves 2 and 3 of Figure 1a also show that some conformers of benzil included into calix[6]arene and calix[8]arene are more planar in the sense that a large conjugation exists, including both pairs of carbonyl and phenyl groups. In Figure 2a, this conjugation can be observed in the new bands which appear at 1662 and 1653 cm^{-1} for benzil/calix[8]arene and benzil/calix-[6]arene complexes, both 1:1 mol ratio. These data are in

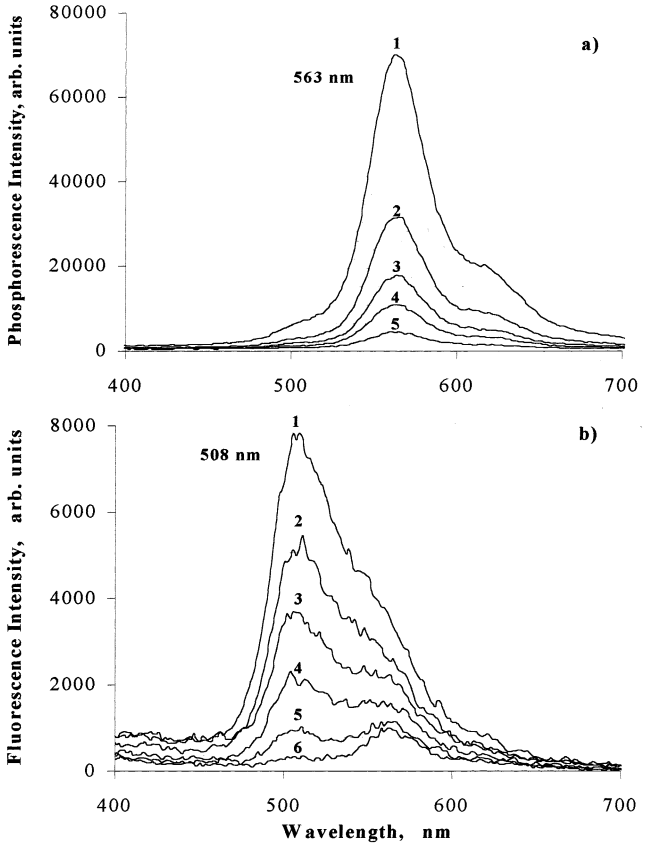

Figure 4. Room-temperature laser-induced luminescence spectra from argon-purged samples of (a) phosphorescence emission from a benzil/silicalite 250 μmol g^{-1} sample. Curves 1, 2, 3, 4, and 5 were recorded 0.1, 100, 300, 500, and 900 μs after laser pulse. (b) Fluorescence emission spectra from the same sample. Curves 1, 2, 3, 4, 5, and 6 were recorded 0.1, 1.0, 2.0, 3.0, 4.0, and 10 ns after laser pulse. λ_{exc} = 337 nm in all cases.

TABLE 1: Carbonyl Stretching Band Wavenumbers Obtained from FTIR Absorption Spectra for Samples of Benzil/Calix[4]arene and Benzil/Calix[*n*]arene Inclusion Complexes for n = 6 and 8, When Compared with Microcrystals of Benzil and Silicalite Channel Inclusion

	$\upsilon_{C=O}$ (cm^{-1})			
microcrystals of BZL	1676; 1659			
mol:mol ratio	1:1	1:2.5	1:5	1:1[a] mec. mix.
BZL/Calix[8]arene	1683; 1675 1662; 1653	1684; 1675	1684; 1675	1674; 1658
BZL/Calix[6]arene	1683; 1672 1662; 1653	1686; 1673	1686; 1673	1675; 1663
BZL/Calix[4]arene	1675; 1660	1674; 1659	1674; 1661	1675; 1660
μmol g^{-1}	1000	500	250	1000 mec. mix.
BZL/Silicalite	1681; 1669	1682; 1668	1683; 1669	1672; 1657

[a] Immediately recorded after mixing.

accordance with the tail in the right-hand of ground-state absorption spectra (Figure 1a).

In the benzil/silicalite samples, the reduced coplanarity between the carbonyl groups and the phenyl groups is kept, as the 1681 and 1669 cm^{-1} stretching vibrations show. Other interesting features that can be observed in Figure 2b are the narrow absorption bands of the carbonyl in the benzil/silicalite samples in comparison with the broad bands observed for benzil/calix[6]arene or calix[8]arene cases. In the former cases, molecules are included into channels of well-defined geometry, while in the latter cases the different conformers of the calix molecules provide different environments, therefore the broadening effects.

TABLE 2: Phosphorescence Emission Lifetimes (longer components) for Samples of Benzil/Calix[4]arene and Benzil/Calix[*n*]arene Inclusion Complexes for n = 6 and 8, When Compared with Microcrystals of Benzil and Silicalite Channel Inclusion

	τ_P (μs)[a]					
microcrystals of BZL at 522 nm	air-equilibrated 145			argon-purged 145		
mol:mol ratio	1:1	1:2.5	1:5	1:1	1:2.5	1:5
BZL/Calix[4]arene at 522 nm	145	145	145	145	145	145
BZL/Calix[6]arene at 563 nm	900	725	725	1000	1000	1000
BZL/Calix[8]arene at 567 nm	145	145	290	245	360	360
μmol g^{-1}	1000	500	250	1000	500	250
BZL/Silicalite at 563 nm	350	290	45	350	350	350

[a] Estimated error ±5%.

Room-Temperature Laser-Induced Phosphorescence. Figure 3a shows the room-temperature phosphorescence spectra of a 1:2.5 mol:mol inclusion complex of benzil and *p-tert*-butylcalix[4]arene ,while Figures 3b and 3c present similar data for *p-tert*-butylcalix[6]arene and *p-tert*-butylcalix[8]arene as hosts. As an excitation source we used the short pulse (600 ps halfwidth, 1.3 mJ per pulse) of a nitrogen laser pulse at 337 nm, quite suitable for benzil time-resolved luminescence studies as a result of its short duration. All time-resolved spectra presented in Figure 3 were obtained with argon-purged samples.

Those samples were also used to record spectra from air equilibrated samples. In the calix[4]arene case, spectra were identical within experimental error, and the same for the lifetimes. However different lifetimes with and without oxygen were obtained for the other two calixarenes, as shown in Table 2 .

A comparison was made of the time-resolved emission spectra from microcrystals of benzil (complex decay, with a small initial fast component ($\tau_P \cong 50$ μs) followed by a longer component of $\tau_P \cong 145$ μs), and the benzil/calix[4]arene inclusion complex time-resolved emission spectra (Figure 3a). Very similar vibrational band structure as well as equal phosphorescence lifetimes were obtained within experimental error, either in the presence or in the absence of oxygen. The time-resolved absorption and emission spectra of microcrystals of benzil were studied in the 1980's by Wilkinson,[36] and described as a mixture of first- and second-order decays (the same decay constants were obtained from absorption and emission decays). This was also verified for our samples, the maximum emission wavelength coincides and is 522 nm. All these data point to the same conclusion: benzil is not included into the calix[4]arene cavity, rather it is deposited on the surface of the powdered solid in the form of microcrystals.

A very different situation was found for the two other calixarene hosts. Benzil exhibits similar spectra and well defined vibrational structure for the complexes with calix[6]arene and calix[8]arene but now with different maximum emission wavelengths at 563 and 567 nm respectively as figures 3b and 3c show. A large deviation of the emission maximum of benzil exists in the case of these two hosts when compared to the microcrystals and calix[4] cases.

This effect is well described for solution studies of benzil.[16,17,21c] The room temperature and low temperature (77 K) solution emission spectra of benzil correspond to "relaxed" and "unre-

laxed" excited states of this probe, respectively. The relaxed excited state has a *s*-trans planar geometry with zero dipole moment, while the unrelaxed form corresponds to a skew conformation both in singlet and triplet states. As a consequence, phosphorescence emission maxima from *s*-trans planar conformers are about 50 nm deviated to the red when compared to the phosphorescence emission from the skew conformers.[16,17]

As we said before, it is well described in the literature that both guest and hosts (calixarenes) exhibit different conformations,[5,6,17,19] and so this fact has to be taken into account in all data analysis.

So, when benzil forms inclusion complexes with calix[6]arene and calix[8]arene, the maxima of phosphorescence emission at room temperature (air-equilibrated or argon-purged samples) are at about 565 nm, showing that the cavities inside the two calixarenes have space enough for the probe to rotate axially and assume *s*-trans planar conformations. At the same time, analysis of Table 2 also shows that calix[6]arene provides the best entrapment conditions, diminishing nonradiative pathways for the excited-state deactivation, therefore increasing the triplet lifetimes and intensities of emission, which are about 1 order of magnitude higher in this calixarene than in calix[8]arene (not shown in Figure 3b).

This change in the benzil lifetime going from *p-tert*-butylcalix[6]arene to *p-tert*-butylcalix[8]arene may also be related with hydrogen abstraction reactions with benzil ketyl radical formation as diffuse-reflectance laser flash photolysis experiments show (data presented in the next section). The more ketone radical is formed, the smaller lifetime for benzil phosphorescence emission was experimentally determined.

In the case of the microcrystals of benzil, the effect of the oxygen is negligible within experimental error, both in terms of the intensity of the phosphorescence emission and lifetimes, suggesting the quenching of a few surface molecules but not of the molecules below the surface of the microcrystals. Laser can excite the latter ones, and since they are not reachable by the oxygen from the air, they can phosphoresce.

We therefore conclude that for solid powdered samples, calixarenes shield only partially the guest from oxygen quenching, at least for the loadings of the guests used in this study.

The benzil emission from silicalite samples (250, 500, and 1000 μmol g^{-1}) is also from a relaxed conformer and is presented in Figure 4a. Lifetimes are similar to the ones detected for calix[8]arene, but an important difference exists: the higher the benzil loading, the smaller the oxygen effect. Benzil molecules block the entrance into the silicalite channels and oxygen is not able to reach the excited molecules, therefore no oxygen quenching effect exists for high loadings.

It is important to point out that, in all the samples referred until now, and apart from the phosphorescence emission, fluorescence emission from a relaxed S1 state was also detected with lifetimes around 2 ns, in accordance with the value reported for this prompt emission.[18] Figure 4b presents this fluorescence emission for benzil within silicalite channels, superimposed on the much longer-lived phosphorescence emission with a maximum at about 563 nm. Similar spectra were also obtained for benzil/calix[6] and [8]arenes. To obtain these time-resolved fluorescence spectra we simply used a nanosecond time gate in our intensified charge coupled device, triggering the detector after laser pulse, rather than introducing a delay after laser pulse for detection, to separate the long-lived emissions from the prompt ones.

A final important remark on the luminescence from benzil/calix[6]arene, silicalite, and calix[8]arene samples regards the existence of some delayed fluorescence which is significative in the calix[6]arene case and decreases in importance in the order silicalite, calix[8]arene (please see Figures 3a, 3b, and 4a), with emission maxima at about 505 nm. This process is thermally activated since it decreases with the decrease of temperature and does not occur at 77 K in all cases. At room temperature, a decay kinetic analysis is possible in the case where this emission is more relevant (benzil/calix[6]arene samples) and shows that the decay rate constant at 505 nm is the same as the one for the triplet emission, within experimental error. This agrees with a thermally activated back intersystem crossing mechanism.[37] If it was a triplet−triplet annihilation (or P-type process) as reported for benzil in benzene,[18] the decay rate constant at 505 nm and at long times should be about two times that found for phosphorescence decay.[37] The existence of several conformations in the calixarenes, and also of the spaces in the intersections of the silicalite channels, could enable the encounter of the excited triplet molecules resulting in the re-formation of the emitting singlet excited species. However, this is not the case for the arguments presented before.

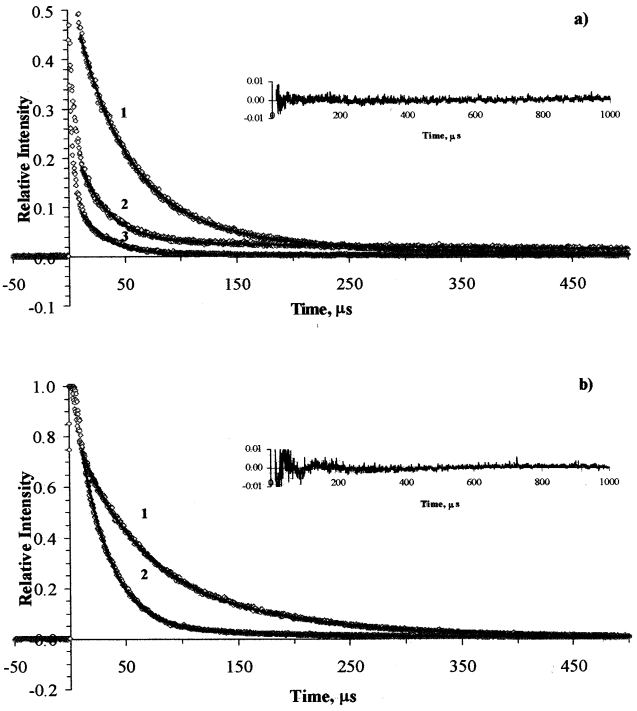

Figure 5. Room-temperature laser-induced luminescence decay curves from air-equilibrated samples of (a) benzil/calix[*n*]arenes 1:2.5 molar ratio samples. Curves 1, 2, and 3 were obtained for $n = 4$, 6, and 8, respectively. (b) Benzil microcrystals (curve 1) and benzil/silicalite 1000 μmol g^{-1} (curve 2). In all curves, the calculated decay is superimposed on the decay trace. The insets exhibit the residuals of the fitting for calix[6]arene as host in part a of the figure and for silicalite as host in part b of the figure.

Kinetic Analysis. Figure 5a and 5b show the room-temperature laser-induced luminescence decay curves from air-equilibrated samples of benzil/calix[*n*]arenes 1:2.5 molar ratio samples (curves 1, 2, and 3 were obtained for $n = 4$, 6, and 8, respectively), and Figure 5b shows the same data for benzil microcrystals (curve 1) and benzil/silicalite 1000 μmol g^{-1} (curve 2). In all cases, samples were excited at 337 nm and monitored at the maximum of the phosphorescence emission of benzil. In all curves, a calculated decay assuming a biexponential decay is superimposed on the decay trace.

Decay curves were analyzed with the Albery's model[34a] since this treatment applies to molecules lying in a variety of surface

TABLE 3: Results from Albery's Model and Two Exponential (least-squares fitting analysis) of Phosphorescence Emission Decay Profiles from Air-Equilibrated Samples of Benzil/Calix[4]arene and Benzil/Calix[*n*]arene Inclusion Complexes for $n = 6$ and 8 (1:2.5 molar ratio), When Compared with Silicalite Channel Inclusion (500 μmol g^{-1}) and Microcrystals of Benzil ($\lambda_{exc} =$ 337 nm in all cases)

	λ_{anal} (nm)	$\bar{k}$ (s^{-1})	γ	τ_1 (μs)	τ_2 (μs)	A_1	A_2
BZL/Calix[4]arene	525	2.40×10^4	0.90	43	145	0.429	0.092
BZL/Calix[6]arene	565	—[a]	—[a]	26	725	1.500	0.021
BZL/Calix[8]arene	565	16.5×10^4	1.8	22	145	0.113	0.008
BZL/Silicalite	565	—[a]	—[a]	27	290	1.026	0.036
Microcrystals of BZL	525	1.45×10^4	0.80	51	145	0.550	0.280

[a] Nonapplicable.

sites, which is certainly the case of benzil on the three calixarenes or within silicalite. This treatment has been successfully employed for time-resolved emission studies of several probes on many surfaces,[32,33] the basic concept being the use of a Gaussian distribution of the free energy change as a suitable description of the heterogeneity of the system. The observed decay profile is a sum of the different contributions to the decay (one probe decaying unimolecularly in different environments). An average rate constant ($\bar{k}$) and a width of the distribution (γ) of the rate constant logarithms can be obtained in the context of this model. The appliance of this approach to an unimolecular decay in homogeneous media provides a width of distribution equal to zero, and a unique rate constant characteristic of the decay.

We know from room-temperature phosphorescence emission studies that benzil emission originates from relaxed conformations (peaking at about 565 nm) and unrelaxed conformations (peaking at about 522 nm). This means that a two exponential analysis of the decays could be applied, although this approach does not take into account the heterogeneity of the surfaces which exist because of the different conformations of the calixarene molecules, different adsorption sites on calix[4]arene surface or silicalite internal structure heterogeneity.

Table 3 presents the values of $\bar{k}$ and γ obtained by using Albery's model to the above-described samples, and it also presents the short-lived and long-lived components obtained from a simple two exponential analysis. These data are consistent with time-resolved phosphorescence spectra presented before and give complementary information in what regards the short-lived emission.

This table clearly shows that the dispersion kinetics only provides a reasonable description of the decay in the cases where microcrystals of benzil emit, and that the simple two-exponential approach provides a more reasonable description despite the heterogeneity of the hosts, since we have emissions from skew and relaxed conformations of benzil. The short and long components may tentatively be assumed to account for the skew and relaxed conformations's emissions, respectively. However, this simple two-exponential analysis for complex systems as the ones we are studying (both guest and host exhibit different conformations,[5,6,17,19]) is clearly a limited tool for a complete kinetic analysis. In this publication we made the option of presenting only this simple analysis, although we are aware of the fact that a lifetime distribution analysis was recently used[34b,c,d] and could also be applied here. It should also be pointed out that lifetime distribution analysis presents instability problems inherent to the mathematical nature of the approach,[34d] and that possible solutions must be determined on the basis of the physical background of the system under study.[34d]

Diffuse Reflectance Laser Flash Photolysis. Time-resolved absorption spectra of samples of benzil/calix[4]arene, of benzil/calix[*n*]arene with $n = 6$ and 8 inclusion complexes and benzil/silicalite samples were obtained by the use of diffuse reflectance laser flash photolysis technique, developed by Wilkinson and co-workers.[25,26] In this study, the use of an intensified charge-coupled device as detector allowed us to obtain time-resolved absorption spectra with nanometer spectral resolution.[9,23]

Figures 6a, 6b, and 6c show the time-resolved absorption spectra of benzil/calix[4]arene, of benzil/calix[*n*]arene with $n = 6$ and 8 inclusion complexes for $n = 6$ and 8, respectively, (molar ratio 1:2.5) and Figure 6d shows similar data for the benzil/silicalite host/guest system. All spectra were obtained for air-equilibrated samples, exciting at 355 nm.

Transient absorption spectra of benzil/*p-tert*-butylcalix[4]-arene samples provide evidence for simultaneous formation of triplet benzil (microcrystals) and also of the phenoxyl radical of calix[4]arene. The triplet−triplet absorption spectrum of microcrystals of benzil is easily identified from comparison with the one published by Wilkinson at al[36] and the one of the phenoxyl radical of calix[4]arene by comparison with previous data reported by us.[9] Phenoxyl radicals of calix[4], [6], and [8]arenes are formed by direct excitation of these molecules at 355 or 266 nm and live at least hundreds of milliseconds, as we reported recently,[9] peaking at 400 and 320 nm. In this sample, the time-resolved absorption spectra peak at about 510 nm both initially and at longer time scales, showing that the absorption is mainly due to the triplet excited state of microcrystals of benzil. Probably some ketyl radical of benzil is also formed with the hydrogen atom released from the calix molecule, but in such a small quantity that it cannot be observed in the transient absorption spectra we show in Figure 6a.

The triplet−triplet transient absorption of benzil (peaking at 482 nm) becomes evident in the cases of *p-tert*-butylcalix[6]-arene and *p-tert*-butylcalix[8]arene inclusion complexes as Figures 6b and 6c clearly show. In these spectra, a new species appears and becomes more evident at longer times (~20 to 100 μs after laser pulse), which peaks at about 370 nm and a shoulder at about 480 nm, characteristic of the benzil ketyl radical absorption.[18,21] The well-known absorption bands of the phenoxyl radical at 400 and 320 nm cannot be observed in this case. So the calix[6] and [8]arenes behave as hydrogen atom donors toward the excited aromatic ketone. The same behavior was detected for the benzophenone/calix[6] and [8]arene inclusion complexes.[9]

The fact that no benzil ketyl radicals were formed in the calix-[4]arene samples, but evidence for ketyl radical formation was obtained in the calix[6]arene and calix[8]arene cases, is obviously related with the fact that, due to the reduced internal space of the calix[4]arene cavity, no inclusion complex is formed. Therefore, no hydrogen abstraction reaction occurs because benzil is simply deposited on the powdered solid external surface in the form of microcrystals, as we observed before in the ground-state absorption and FTIR studies.

Inside the silicalite channels, benzil finds no suitable hydrogen atom donor and only the triplet−triplet T1 → T2 transient absorption of this aromatic ketone was observed, peaking at 492 nm. This value is similar to that determined for benzil transient absorption in nonpolar solvents such as benzene or liquid paraffin.[21,38] As we saw before, in high loadings of benzil (1000 μmol g^{-1}) this guest blocks the oxygen entrance. This also means that in this host, benzil probably has a much more reduced photochemical reactivity.

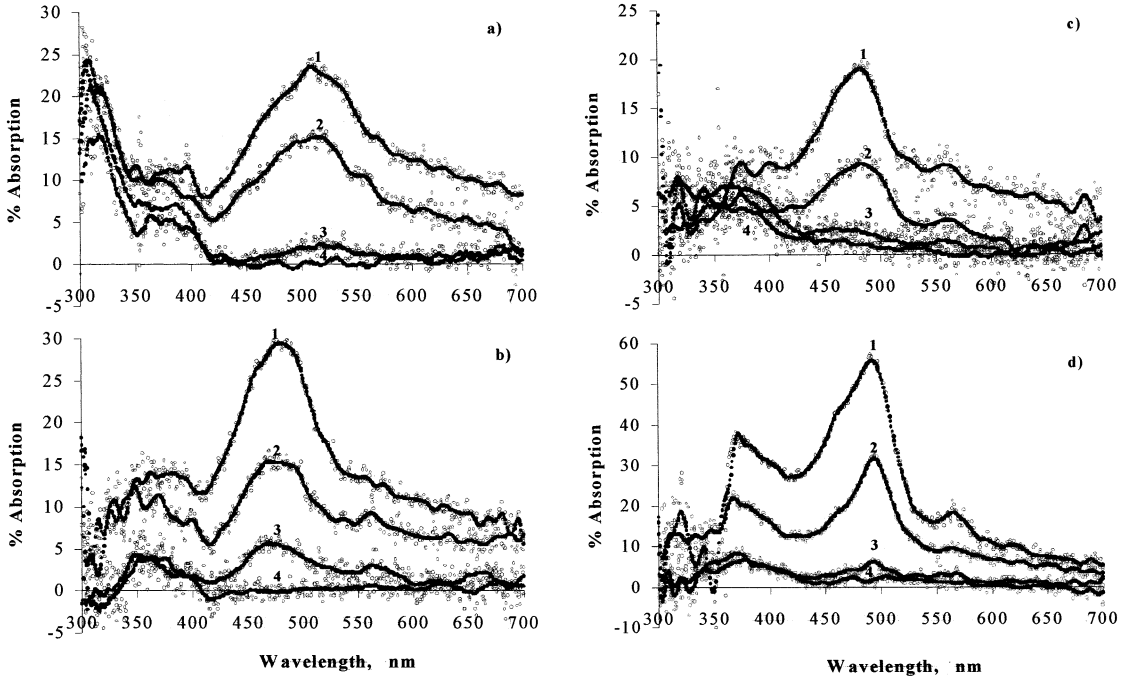

Figure 6. (a) Time-resolved absorption spectra of benzil/calix[4]arene sample (molar ratio 1:2.5). Curves 1, 2, 3, and 4 were recorded 1, 5, 100 μs, and 20 ms after laser pulse. (b) Time-resolved absorption spectra of benzil/calix[6]arene inclusion complex (molar ratio 1:2.5). Curves 1, 2, 3, and 4 were recorded 1, 5, 20 μs, and 20 ms after laser pulse. (c**)** Time-resolved absorption spectra of benzil/calix[8]arene inclusion complex (molar ratio 1:2.5). Curves 1, 2, 3, and 4, were recorded 0.5, 5, 20 μs, and 20 ms after laser pulse. (d) Time-resolved absorption spectra of benzil/silicalite 250 μmol g^{-1} sample. Curves 1, 2, 3, and 4 were recorded 0.03, 10, 100 μs, and 20 ms after laser pulse. $\lambda_{exc} = 355$ nm in all cases.

However, it is important to point out that, at very long times ($\geq$20 ms), a residual transient absorption is still detected (see curve 4 of Figure 6d). This transient peaks at about 370 nm and shows a kind of long absorption "tail" which finishes at about 700 nm. By comparison with the transient absorption spectra reported in acetonitrile (a poor photoreducing agent), we assign this transient as being the benzoyl radical, resulting from the α-cleavage reaction of benzil.[39,40] Further studies of photodegradation of benzil support this assignment, as we will see in the next section.

Photodegradation Products Studies. Solution photochemistry reactions of benzil have been studied by flash photolysis and were mainly reported by Scaiano et al.[20] They can be briefly described by the following scheme:

$$\text{Ph-CO}-\text{CO}-\text{Ph} \xrightarrow{h\nu} {}^1(\text{Ph-CO}-\text{CO}-\text{Ph})^* \qquad (1)$$

$${}^1(\text{Ph-CO}-\text{CO}-\text{Ph})^* \rightarrow {}^3(\text{Ph-CO}-\text{CO}-\text{Ph})^* \qquad (2)$$

$${}^3(\text{Ph-CO}-\text{CO}-\text{Ph})^* \rightarrow {}^3\,2\ \text{Ph-C}^{\bullet}\text{O} \qquad (3)$$

$${}^3(\text{Ph-CO}-\text{CO}-\text{Ph})^* \xrightarrow{+\text{H}^{\bullet}} \text{Ph-C}^{\bullet}\text{OH}-\text{CO}-\text{Ph} \qquad (4)$$

Reaction 3 describes the formation of the benzoyl radical (Norrish type I cleavage) following laser excitation, and reaction 4 the formation of the benzil ketyl radical (intermolecular hydrogen atom abstraction).[20,21] Photoreduction of benzil originates, in general, benzil ketyl radicals in nonpolar solvents and the radical anion in hydroxylic media.[20a] This latter species is easily identified since its transient absorption peaks at about 600 nm,[21] so we can be confident that the radical anion is not formed in our cases.

One can expect reactions 3 and 4 to occur in the reverse direction with the re-formation of the starting materials or subsequent second hydrogen atom abstraction with benzaldehyde and benzoin formation, respectively.

Following laser excitation (266 or 355 nm) or steady-state lamp irradiation (254 nm), product analysis, and identification was attempted. Under lamp irradiation conditions microcrystals of benzil were found to be quite stable. Benzil photoreactions in silicalite and calix[4]arene are much slower than in the calix[6] and [8]arenes. This was expected from luminescence and transient absorption results of calix[4]arene, due to the fact that inclusion does not occur and the so formed microcrystals (adsorbed on the calix[4] surface) are stable. The reduced photochemical reactivity found in silicalite is in accordance with its transient absorption, which is mainly due to the triplet−triplet absorption. Being an inert support, silicalite does not supply any simple degradation pathway to the transients formed after laser excitation.

HPLC and GC-MS analysis clearly showed that the main degradation products in all substrates can be rationalized as being reaction derivatives of the benzoyl radical. In the silicalite case, the identified products were benzaldehyde and methyl benzoate when the extraction from the irradiated sample was made with methanol, or ethyl benzoate if ethanol was used. The same solvent dependence was found for all the other solid supports. Hydrogen abstraction from the solvent leads to benzaldehyde and the further recombination of the resulting alkoxyl radical with another benzoyl radical leads to the corresponding benzoate (see Scheme 2). This result confirms the assignment made of the long-lived species observed in all substrates and indicates that benzoyl radicals have half-lives of minutes at the least.

In contrast with the solution behavior, where α-cleavage of benzil is achieved only by a two-photon process,[20c] in the solids under study, this is the main degradation pathway. In calix[6] and [8]arenes cases, a residual concentration of benzoin was also detected. This compound, which was previously reported

SCHEME 2

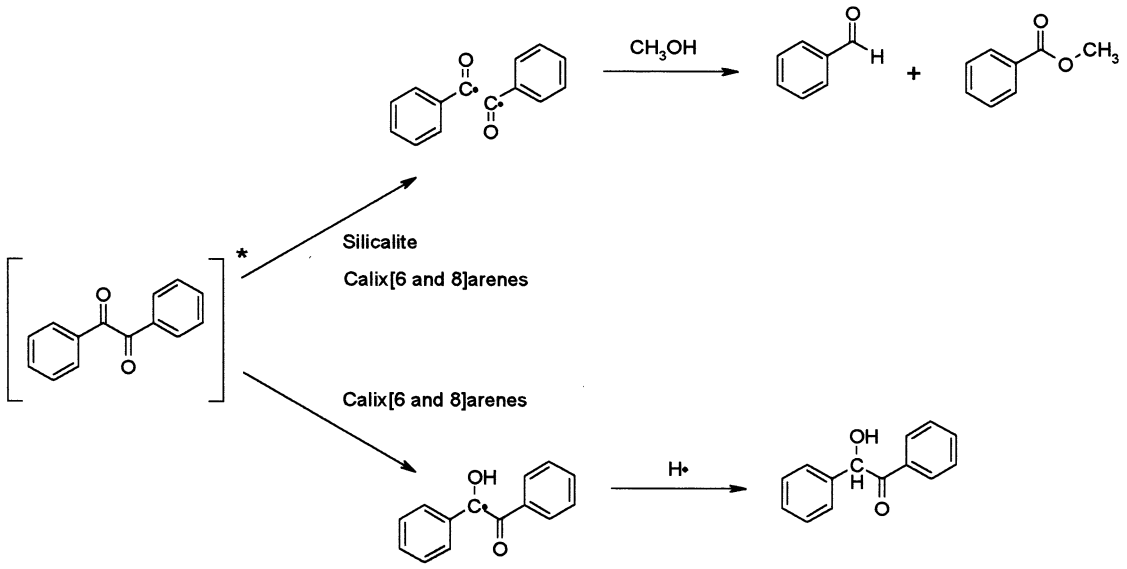

to be a photodegradation product of benzil,[41] can be formed by a hydrogen abstraction of the benzil ketyl radical from the hosts. Transient absorption spectra indicated the presence of this radical in the cases where inclusion complexes were formed. The low concentration of benzoin can be due to photodegradation since its dissociation yields were found to be relatively high.[42] This compound is even used as a good photoinitiator for radical polymerization.[43] Calix[6] and [8]arenes are able to supply the hydrogen atoms which enable the reaction channel which leads to benzoin through benzyl ketyl radicals formation, as Scheme 2 shows. Other identified photoproducts were benzophenone, 2-hydroxy benzophenone, phenylbenzoate, and biphenyl. Most of these products can be accounted for by benzoyl radical reactions (decarbonylation and radical coupling) and/or photodegradation of the primary degradation products of benzil. All identifications were based on the analysis of authentic samples and/or GC-MS and UV−Vis spectra.

4. Conclusions

Inclusion of benzil into different hosts, namely *p-tert*-butylcalix[6]arene, *p-tert*-butylcalix[8]arene, and silicalite, results in significative changes both in ground-state absorption spectra as well as time-resolved emission and absorption spectra. *p-tert*-Butylcalix[4]arene does not include the benzil molecule which stays deposited on the surface of the powdered solid in the form of microcrystals.

In the calix[6]arene and calix[8]arene cases the probe is in hydrophobic and constrained environments, which exhibit a certain polarity. These calixarenes exhibit multiple conformations which promote the interactions of the carbonyl group of the ketone and the hydroxyl groups of the calixarene. Silicalite as a host provides the most rigid and nonpolar environment for the ketones, the internal cavities being zigzag channels which intersect. In the former case, photochemical reactions occur with ketyl and benzoyl radical formation and in the latter only benzoyl radical transient absorption was detected. In all cases, triplet−triplet absorption of benzil was also detected.

Product analysis and identification show that the main detected degradation products in all substrates are benzoyl radical derivatives. The identified products were benzaldehyde and methyl benzoate if the extraction from the irradiated sample was made with methanol or ethyl benzoate whenever ethanol was used. Calix[6] and [8]arenes are able to supply hydrogen atoms which allow another reaction channel to occur, which leads to benzoin through benzil ketyl radicals formation.

Acknowledgment. Equipment was financed by project Praxis/P/Qui/10023/98. The authors thank ICCTI/CAPES for financial support. A.S.O. and J.P.S. thank FCT for Postdoctoral fellowships SFRH/BPD/36500/2000 and SFRH/BPD/15589/2001.

References and Notes

(1) (a) Gutshe, C. D. *Calixarenes*; Royal Society of Chemistry: Cambridge, U.K., 1989. (b) Gutshe, C. D. *Calixarenes Revisited, Monographs in Supramolecular Chemistry*; Royal Society of Chemistry: Cambridge, U.K., 2000. (c) Gutsche, C. D. *Aldrichim. Acta* **1995**, 28, 3−9.

(2) Atwood, J. L.; Koutsantonis, G. A.; Raston, C. L. *Nature* **1994**, *368*, 229−231.

(3) (a) Shinkai, S.; Ikeda, A. *Pure Appl. Chem.* **1999**, *71*, 275−280. (b) Suzuki, T.; Nakashima, K.; Shinkai, S. *Chem. Lett.* **1994**, 699−702.

(4) Perrin, R.; Lamartine, R.; Perrin, M. *Pure Appl. Chem.* **1993**, *65*, 1549−1559.

(5) Lazzarotto, M.; Nachtigal, F. F.; Nome, F. *Quim. Nova* **1995**, *18*, 444−453.

(6) Ikeda, A.; Shinkai S. *Chem. Rev.* **1997**, *97*, 1713−1734.

(7) Alam, I.; Gutsche, C. D. *J. Org. Chem.* **1990**, *55*, 4487−4489.

(8) Gutsche, C. D.; Alam, I. *Tetrahedron* **1988**, *44*, 4689−4694.

(9) Vieira Ferreira, L. F.; Vieira Ferreira, M. R.; Oliveira, A. S.; Branco, T. J. F.; Prata, J. V.; Moreira, J. C. *Phys. Chem. Chem. Phys.* **2002**, *4*, 204−210.

(10) Barra, M.; Agha, K. A. *Supramol. Chem.* **1998**, *10*, 91−95.

(11) (a) Shi, Y.; Zhang, Z. *J. Chem. Soc., Chem. Commun.* **1994**, 375−376. (b) Shi, Y.; Wang, D.; Zhang, Z. *J. Photochem. Photobiol.* **1995**, *91*, 211−215.

(12) Huang, F.; Yang, J.; Hao, A.; Wu, X.; Liu, R.; Ma, Q. *Spectrochim. Acta A* **2001**, *57*, 1025−1030.

(13) (a) Bourdelande, J. L.; Font, J.; González-Moreno, R.; Nonell, S. *J. Photochem. Photobiol. A: Chem.* **1998**, *115*, 69−71. (b) Bourdelande, J. L.; Font, J.; González-Moreno, R. *J. Photochem. Photobiol. A: Chem.* **1996**, *94*, 215−216.

(14) Tung, C. H.; Ji, H. F. *J. Chem. Soc., Perkin Trans. 2* **1997**, 185−188.

(15) Liu, Y.; Han, B. H.; Chen, Y. T. *J. Org. Chem.* **2000**, *65*, 6227−6230.

(16) Morantz, D. J.; Wright, A. J. C. *J. Chem. Phys.* **1971**, *54*, 692−697.

(17) (a) Bhattacharyya, K.; Chowdhury, M. *J. Photochem.* **1986**, *33*, 61−65. (b) Bera, S. C.; Mukherjee, R.; Chowdhury, M. *J. Phys. Chem.* **1969**, *51*, 754−761.

(18) Okutsu, T.; Ooyama, M.; Tani, K.; Hiratsuka, H.; Kawai, A.; Obi, K. *J. Phys. Chem. A* **2001**, *105*, 3741−3744.

(19) Fessenden, R. W.; Carton, P. M.; Shimamori, H.; Scaiano, J. C. *J. Phys. Chem.* **1982**, *86*, 3803−3811.
(20) (a) Scaiano, J. C. *J. Phys. Chem.* **1981**, *85*, 2851−2855. (b) Encinas, M. V.; Scaiano, J. C. *J. Am. Chem. Soc.* **1979**, *101*, 7740−7741. (c) McGimpsey, W. G.; Scaiano, J. C. *J. Am. Chem. Soc.* **1987**, *109*, 2179−2181.
(21) (a) Mukai, M.; Yamaushi, S.; Hirota, N. J. *J. Phys. Chem.* **1992**, *96*, 3305−3311. (b) *J. Phys. Chem.* **1992**, *96*, 9328−9331. (c) *J. Phys. Chem.* **1992**, *93*, 4411−4413.
(22) (a) Flaningen, E. C.; Bennet, J. M.; Grose, R. W.; Patton, R. L.; Kirchner, R. M.; Smith, J. V. *Nature* **1978**, *271*, 512−516. (b) Shultz-Sibbel, G. M. W.; Gjerde, D. T.; Chriswell, C. D.; Fritz, J. S.; Colleman, W. E. *Talanta* **1982**, *29*, 447−452. (c) Bibby, D. M.; Millestone, N. B.; Aldridge, L. P. *Nature* **1979**, *280*, 664−665.
(23) (a) Vieira Ferreira, L. F. *Química* **1999**, *72*, 28−46. (b) Botelho do Rego, A. M.; Vieira Ferreira, L. F. In *Handbook of Surfaces and Interfaces of Materials*; Nalwa, H. S., Ed.; Academic Press: New York, 2001; Vol. 2, Chapter 7, pp 275−313.
(24) Vieira Ferreira, L. F.; Netto-Ferreira, J. C.; Khmelinskii, I.; Garcia, A. R.; Costa, S. M. B. *Langmuir* **1995**, *11*, 231−236.
(25) Wilkinson, F.; Kelly, G. P. In *Photochemistry on Solid Surfaces*; Anpo, M., Matsuara, T., Eds.; Elsevier: Amsterdam, 1989; pp 31−47.
(26) Wilkinson, F.; Kelly, G. P. In *Handbook of Organic Photochemistry*; Scaiano, J. C., Ed.; CRC Press: Boca Raton, FL, 1989; Vol. 1, Chapter 12, pp 293−314.
(27) (a) Vieira Ferreira, L. F.; Freixo, M. R.; Garcia, A. R.; Wilkinson, F. *J. Chem. Soc., Faraday Trans.* **1992**, *88*, 15−22. (b) Vieira Ferreira, L. F.; Garcia, A. R.; Freixo, M. R.; Costa, S. M. B. *J. Chem. Soc., Faraday Trans.* **1993**, *89*, 1937−1944.
(28) Hurtubise, J. H. *Anal. Chim. Acta* **1997**, 351, 1−22.
(29) Oliveira, A. S.; Fernandes, M. B.; Moreira, J. C.; Vieira Ferreira, L. F. *J. Bras. Chem. Soc.* **2002**, *13*, 245−250.
(30) (a) Da Silva, J. P.; Da Silva, A. M.; Khmelinskii; I. V.; Martinho, J. M. G.; Vieira Ferreira, L. F. *J. Photochem. Photobiol. A: Chem.* **2001**, *142*, 31−37. (b) Da Silva, J. P.; Vieira Ferreira, L. F.; Da Silva, A. M.; Oliveira, A. S. *J. Photochem. Photobiol. A: Chem.* **2002**, *151*, 157−164.
(31) Leigh, W. J.; Johnson, L. J. In *Handbook of Photochemistry*; Scaiano, J. C., Ed.; CRC Press: Boca Raton, FL, 1989; Chapter 22, pp 401−422.
(32) (a) Mao, Y.; Thomas, J. K. *J. Chem. Soc., Faraday Trans.* **1992**, *88*, 3079−3086. (b) Mao, Y.; Zang, G.; Thomas, J. K. *Langmuir* **1993**, *9*, 1299−1305.
(33) (a) Mao, Y.; Thomas, J. K. *Langmuir* **1992**, *8*, 2501−2508. (b) Thomas, J. K. *Chem. Rev.* **1993**, *93*, 301−320.
(34) (a) Albery, W. J.; Bartlett, P. N.; Wilde, C. P.; Darwent, J. R. *J. Am. Chem. Soc.* **1985**, *107*, 1854−1858. (b) Barra, M.; Scaiano, J. C. *Photochem. Photobiol.* **1995**, *62*, 60−64. (c) Sikorski, M.; Sikorski, E.; Khmelinsky, I. V.; Gonzalez-Moreno, R.; Bordelande, J. L.; Siemiarczuk, A. *Photochem. Photobiol. Scien.* **2002**, *1*, 715−720. (d) Liu, T. S.; Ware, W. R. *J. Phys. Chem.* **1993**, *97*, 5980−5986; *J. Phys. Chem.* **1993**, *97*, 5995−6001.
(35) Bellamy, L. J. In *The Infrared Spectra of Complex Molecules*, 2nd ed.; Chapman and Hall: London, 1980; Vol. 2, p 137.
(36) Wilkinson, F.; Willsher, C. J. *Appl. Spectrosc.* **1984**, *39*, 897−901.
(37) Wilkinson, F.; Kelly, G. P.; Vieira Ferreira, L. F.; Freire, V.; Ferreira, M. I. *J. Chem. Soc., Faraday Trans.* **1991**, *87*, 547−552.
(38) Carmichael, I.; Hug, G. L.; Murov, S. L. In *Handbook of Photochemistry*; Marcel Dekker Inc.: New York, 1992.
(39) Fischer, H.; Baer, R.; Hany, R.; Verhoolen, I.; Walbiner, M. *J. Chem. Soc., Perkin Trans. 2* **1990**, 787−798.
(40) Knolle, W.; Muller, U.; Mehnert, R. *Phys. Chem. Chem. Phys.* **2000**, *2*, 1425−1430.
(41) Vijaikumar, S.; Somasundaram, N. K.; Srinivasan, C. *Appl. Catal. A-Gen* **2002**, *223*, 129−135.
(42) Shrestha, N. K.; Yagi, E. J.; Takatori, Y.; Kawai, A.; Kajii, Y.; Shibuya, K.; Obi, K. *J. Photochem. Photobiol. A* **1998**, *116*, 179−185.
(43) Ledwith, A.; Russell, P. J.; Sutcliffe, L. H. *J. Chem. Soc., Perkin Trans. 2, Part II* **1972**, 1925−1928.